Transmission-Line Fault Analysis Using Synchronized Sampling

Papiya Dutta, *Student Member, IEEE*, Ahad Esmaeilian, *Student Member, IEEE*, and
Mladen Kezunovic, *Fellow, IEEE*

Abstract—An automated analysis approach, which can automatically characterize fault and subsequent relay operation, is the focus of this paper. It utilizes synchronized samples captured during transients from both ends of the transmission line to detect, classify, and locate transmission-line faults and can verify that the tripped line has indeed experienced a fault. The proposed method is tested for several faults simulated on an IEEE 118-bus test system and it has been concluded that it can detect and classify a fault using prefault and postfault recorded samples within 7 ms of fault inception and can accurately locate a fault with 3% accuracy. This time response performance is highly desirable since with the increasing use of modern circuit breakers, which can open the faulty line in less than two cycles, the time window of the captured waveforms is significantly reduced due to the unavailability of measurement signals after breakers open.

Index Terms—Electromagnetic transients, fault detection, fault location, power system faults, power system protection.

I. INTRODUCTION

TRANSMISSION lines exposed to different weather, as well as human and animal contacts are subject to several types of faults, which are random and unpredictable. Quick fault analysis to facilitate timely restoration of service when the relay trip is issued due to relay misoperation is a desirable self-healing feature. A fault analysis tool should be able to detect the fault event by automatically interpreting recorded transients captured during relay trip operation.

Several fault analysis methods that are either a complete tool or separate fault detection, classification, and location functions are described in the literature.

Early fault detection and classification techniques were based on changes on voltages, currents, and impedances with respect to some preset values to identify fault types [1], [2]. In the last two decades, different artificial-neural-network (ANN) and fuzzy-based methods were introduced for fault detection and classification [3]–[5]. In general, irrespective of the wide range of operating conditions (varying system loading, fault resistance, fault inception instance, etc.), ANN-based methods have been successful in detecting and classifying the faults,

but they need a huge amount of training cases to achieve good performance. A combination of fuzzy set and wavelet transform method based on line current [6], while using simple fuzzy rules even in case of complex networks, cannot classify all types of faults. In [7], a setting-free two-end method compares the direction of the power measured at two ends and detects and classifies the fault using established rules. Though the method is a setting-free one, calculating the average value of power will cause delay in operation of the method, which can be considered a major drawback if relay operation has to be corrected immediately.

Transmission-line fault-location methods either use power frequency components of voltage and current or higher frequency transients generated by the fault [8], [9]. All of these methods can be subdivided depending upon the availability of recorded data: single-end methods [10]–[12] where data from only one terminal of the transmission line are available and double-end methods [13]–[17] where data from both (or multiple) ends of the transmission line can be used. Double-ended methods can use synchronized or unsynchronized phasor measurements or samples. These methods are suitable for offline analysis but require better computational performance to be used for online analysis.

A typical fault analysis tool [18]–[21] performs fault detection, classification, and location as a total package. In [18], fault detection and classification require some preset thresholds and fault location is based on a less accurate lumped parameter model. In [19], a method that implements fault detection and classification based on the fuzzy ART neural network needs significant training beforehand. The fault-location approach introduced in [19] is very accurate but requires a high sampling rate for input data. The methods introduced in [20] and [21] are based on data captured using the phasor measurement unit (PMU) and, therefore, still depend on phasor calculation, which can cause a delay in obtaining results.

An automated fault analysis tool that overcomes time response and accuracy shortcomings of the previous methods is proposed in this paper. The next section contains a discussion of the proposed method with a mathematical representation for different types of faults and different line configurations. The implementation procedure is discussed next and follows with a summary of test results.

II. PROPOSED METHOD FOR FAULT DETECTION, CLASSIFICATION, AND LOCATION

To detect and classify a fault, the proposed method compares the change of direction of instantaneous powers on all three

This article has been accepted for inclusion in a future issue of this journal. Content is final as presented, with the exception of pagination.
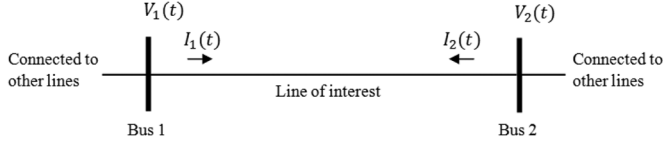
2

IEEE TRANSACTIONS ON POWER DELIVERY

Fig. 1. Transmission line with two-end measurements.

phases computed at two ends of a transmission line using synchronized voltage and current samples measured at both ends. The method has a significant advantage over the method proposed in [7] since computing instantaneous power does not need any averaging and, therefore, the captured samples can be used directly. After a fault is detected and classified, the time-domain-based location method proposed in [17] is used. The fault-location method in [17] requires a high sampling of data while the method used for fault detection and classification requires a lower sampling rate. A spline interpolation technique [22] is used to introduce samples in between two adjacent samples of original voltage and current waveforms, thereby increasing the sampling rate for input data.

A. Fault Detection and Classification

The fault detection and classification method works on comparing the change of sign of magnitudes of instantaneous power computed at two ends of a transmission line using time-synchronized voltage and current samples synchronously measured at both ends.

In Fig. 1, $V_1(t), I_1(t)$ represents the voltage and current measured at one end (Bus 1) of the line at instant t. Similarly, $V_2(t), I_2(t)$ represents voltage and current measured at the other end (Bus 2) of the line at the same instant t. Currents are measured in the assumed direction shown in Fig. 1. All voltage and currents are single-phase quantities.

Voltage and currents at bus 1

$$V_1(t) = V_{1m} \cos \omega t, \quad I_1(t) = I_{1m} \cos(\omega t - \theta_1)\theta_1$$

is a phase angle between $V_1(t)$ and $I_1(t)$.

Instantaneous power at bus 1

$$P_1(t) = V_1(t) \times I_1(t)$$
$$= V_{1m} I_{1m} \cos \omega t \cos(\omega t - \theta_1)$$
$$= P_{1m}(\cos 2\omega t + 1) \cos \theta_1 + P_{1m} \sin 2\omega t \sin \theta_1$$

Voltage and currents at bus 2

$$V_2(t) = V_{2m} \cos(\omega t - \delta), \quad I_2(t) = I_{2m} \cos(\omega t - \delta - \theta_2)\theta_2$$

is the phase angle between $V_2(t)$ and $I_2(t)$. δ is the power factor angle between Bus 1 and Bus 2.

Instantaneous power at bus 2

$$P_2(t) = V_2(t) \times I_2(t)$$
$$= P_{2m}(\cos 2(\omega t - \delta) + 1) \cos \theta_2 .$$
$$+ P_{2m} \sin 2(\omega t - \delta) \sin \theta_2$$

Now with the assumed direction of currents, the magnitude of $I_2(t)$ is negative before the fault and positive after the fault.

For the unfaulted situation, instantaneous powers (superscript "u") are

$$P_1^u(t) = P_{1m}^u(\cos 2\omega t + 1) \cos \theta_1^u + P_{1m}^u \sin 2\omega t \sin \theta_1^u$$
$$P_2^u(t) = -P_{2m}^u(\cos 2(\omega t - \delta) + 1) \cos \theta_2^u$$
$$- P_{2m}^u \sin 2(\omega t - \delta) \sin \theta_2^u .$$

After fault, instantaneous powers (superscript "f") are

$$P_1^f(t) = P_{1m}^f(\cos 2\omega t + 1) \cos \theta_1^f + P_{1m}^f \sin 2\omega t \sin \theta_1^f$$
$$P_2^f(t) = P_{2m}^f(\cos 2(\omega t - \delta) + 1) \cos \theta_2^f$$
$$+ P_{2m}^f \sin 2(\omega t - \delta) \sin \theta_2^f .$$

If the before fault and after fault power factor angles are lagging, that is, $\theta_1^u > 0$, $\theta_2^u > 0$; $\theta_1^f > 0$, $\theta_2^f > 0$, then before fault $|P_1^u(t)| > 0$, $|P_2^u(t)| < 0$ and after fault $|P_1^f(t)| > 0$, $|P_2^f(t)| > 0$.

If before the fault, the power factor angles are leading and postfault power factor angles are lagging, that is, $\theta_1^u < 0$, $\theta_2^u < 0$, $\theta_1^f > 0$, $\theta_2^f > 0$, then before fault

$$|P_1^u(t)| > 0 \text{ if } (\cos 2\omega t + 1) \cos \theta_1^u > \sin 2\omega t \sin \theta_1^u$$
$$|P_2^u(t)| < 0 \text{ if } (\cos 2(\omega t - \delta) + 1) \cos \theta_2^u$$
$$> \sin 2(\omega t - \delta) \sin \theta_2^u$$

and after fault $|P_1^f(t)| > 0$, $|P_2^f(t)| > 0$.

This can be shown in all combinations of lagging and leading power factor angles before and after the fault $|P_1^u(t)| > 0$, $|P_2^u(t)| < 0$, and $|P_1^f(t)| > 0$, $|P_2^f(t)| > 0$ if one or some of the inequalities are true

$$(\cos 2\omega t + 1) \cos \theta_1^u > \sin 2\omega t \sin \theta_1^u \qquad (1)$$
$$(\cos 2(\omega t - \delta) + 1) \cos \theta_2^u > \sin 2(\omega t - \delta) \sin \theta_2^u \qquad (2)$$
$$(\cos 2\omega t + 1) \cos \theta_1^f > \sin 2\omega t \sin \theta_1^f \qquad (3)$$
$$(\cos 2(\omega t - \delta) + 1) \cos \theta_2^f > \sin 2(\omega t - \delta) \sin \theta_2^f . \qquad (4)$$

Under small values of power factor angles, all of the inequalities are satisfied. Generally, in transmission systems, prefault power factor angles are very small and postfault, they are lagging, which is sufficient to conclude

$$|P_1^u(t)| > 0, \ |P_2^u(t)| < 0, \ \left|P_1^f(t)\right| > 0, \ \left|P_2^f(t)\right| > 0. \qquad (5)$$

This article has been accepted for inclusion in a future issue of this journal. Content is final as presented, with the exception of pagination.

DUTTA *et al.*: TRANSMISSION-LINE FAULT ANALYSIS USING SYNCHRONIZED SAMPLING

3

Fig. 2. (a)–(c) $P_1(t)$ and $P_2(t)$ with respect to time for the "ag" fault. (d)–(f) $P\mathrm{sgn}(t)$ with respect to time for the "ag" fault.
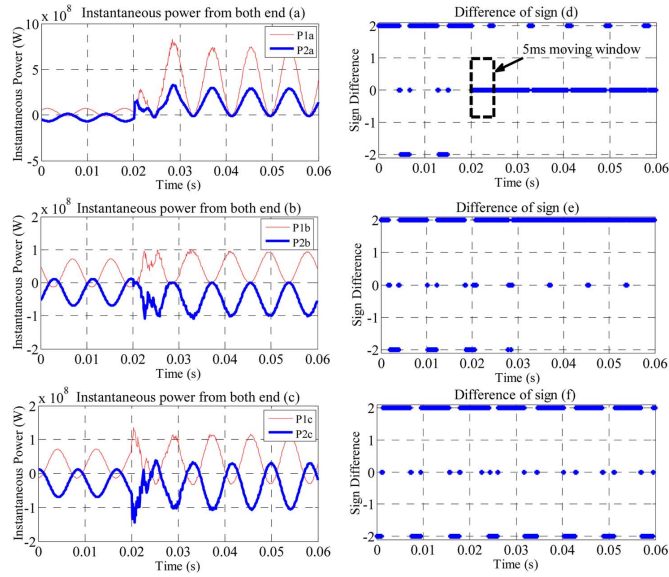

Fig. 3. (a)–(c) $P_1(t)$ and $P_2(t)$ with respect to time for the "ab" fault. (d)–(f) $P\mathrm{sgn}(t)$ with respect to time for the "ab" fault.

Therefore, this is a unique feature of instantaneous power under different types of faults which helps detect and classify faults without using any threshold. This feature is observed only on the faulted phases.

In the following sections, we will use this concept and show how it can be used to detect and classify different types of faults.

1) Single-Phase-to-Ground Fault: In case of the single-phase-to-ground fault (ag), the plot of $P_1(t)$ and $P_2(t)$ with respect to time is shown in Fig. 2(a)–(c). Right after the fault inception (0.02 s), in phase "a," $|P_{1a}^f(t)| > 0$, $|P_{2a}^f(t)| > 0$ while for the other two phases $|P_{1b}^f(t)| > 0$, $|P_{2b}^f(t)| < 0$, $|P_{1c}^f(t)| > 0$, and $|P_{2c}^f(t)| < 0$.

To represent this feature mathematically, the signum function is used, which is defined as

$$\mathrm{sgn}(x) = \begin{cases} -1, & x < 0 \\ 0, & x = 0 \\ 1, & x > 0 \end{cases}.$$

$\mathrm{sgn}(P_1(t))$ and $\mathrm{sgn}(P_2(t))$ are calculated for each phase and the difference $P\mathrm{sgn}(t) = \mathrm{sgn}(P_1(t)) - \mathrm{sgn}(P_2(t))$ for each phase is plotted in Fig. 2(d)–(f). Theoretically, before fault $P\mathrm{sgn}(t)$ should be ± 2 and after fault $P\mathrm{sgn}(t)$ should be 0, but due to the power factor angle and transients and noise present in the measurements, some outliers are present. It is clear from Fig. 2(d)–(f) that on phase "a" $P\mathrm{sgn}(t)$ becomes almost zero after the fault while other phases remain unchanged.

The instant this change occurred is the fault instant. A moving window (5 ms used here) is used to check whether at least 90% (due to the presence of outliers) of $P\mathrm{sgn}(t)$ are zero, which indicates the instant the faulted phase (phase "a" here) experienced a fault.

2) Phase Faults:

a) Phase-to-Phase Fault: In the case of the phase-to-phase fault (ab), the plot of $P_1(t)$ and $P_2(t)$ with respect to time is
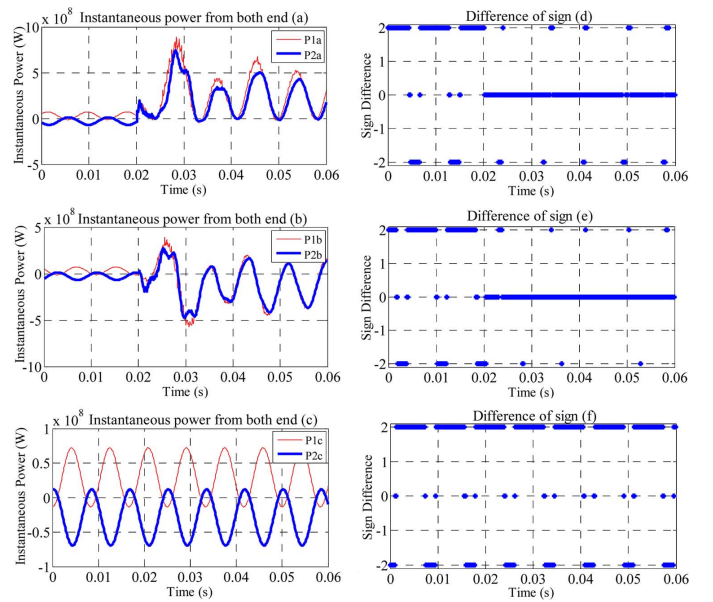
shown in Fig. 3(a)–(c). Right after the fault inception (0.02 s), in phases "a" and "b," $|P_{1a}^f(t)| > 0$, $|P_{2a}^f(t)| > 0$, $|P_{1b}^f(t)| > 0$, $|P_{2b}^f(t)| > 0$, and in phase "c" $|P_{1c}^f(t)| > 0$, $|P_{2c}^f(t)| < 0$. The plot of $P\mathrm{sgn}(t)$ with respect to time is shown in Fig. 3(d)–(f).

It is clear that after the fault $P\mathrm{sgn}(t)$ is almost zero for both phases "a" and "b." Therefore, we can use the same logic used for the "ag" fault to detect the fault in phase-to-phase faults.

b) Phase-Phase-to-Ground Fault: In case of the phase-to-phase-to-ground fault (abg), the plot of $P_1(t)$ and $P_2(t)$ with respect to time is shown in Fig. 4(a)–(c). The plot of $P\mathrm{sgn}(t)$, with respect to time, is shown in Fig. 4(d)–(f). Both plots show exactly the similar behavior as that of the phase-to-phase fault (ab).

As in a phase-to-phase-to-ground fault, a significant amount of zero-sequence current will be present, and it can be used as a classification feature between phase-to-phase and phase-to-phase-to-ground faults.

We define zero-sequence current factors for each phase as

$$F_a = 3I_0(t)/I_a(t), \ F_b = 3I_0(t)/I_b(t), \ F_c = 3I_0(t)/I_c(t)$$

where $3I_0(t) = I_a(t) + I_b(t) + I_c(t)$

Fig. 5(a)–(c) shows the plot of zero-sequence current factors for each phase for the "ab" fault. Fig. 5(d)–(f) shows the same for the "abg" fault. It is clear that those factors are much higher in the case of the "abg" fault. For mathematical implementation, we have rounded those factors and they are always zero for the "ab" fault and greater than zero for the "abg" fault. Therefore, by investigating these factors, classification between the "ab" and "abg" fault is possible.

3) Three-Phase Fault: In case of the three-phase fault (abc), the plot of $P_1(t)$ and $P_2(t)$ with respect to time is shown in
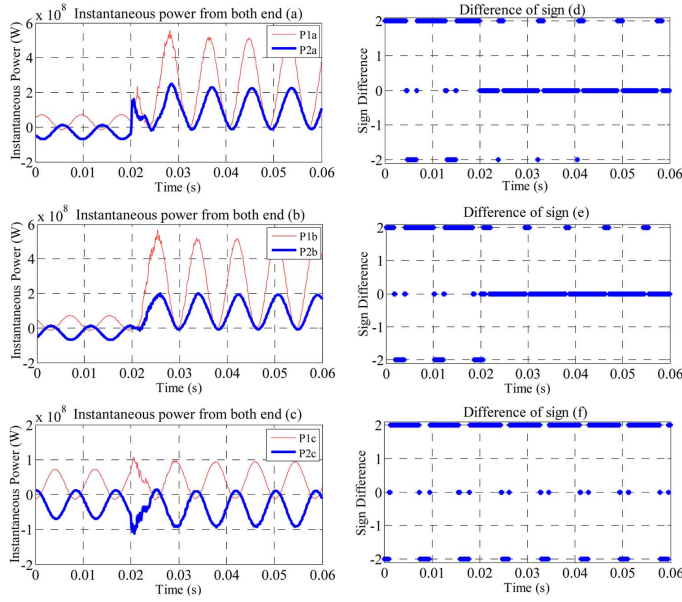
This article has been accepted for inclusion in a future issue of this journal. Content is final as presented, with the exception of pagination.

4   IEEE TRANSACTIONS ON POWER DELIVERY

Fig. 4. (a)–(c) $P_1(t)$ and $P_2(t)$ with respect to time for the "abg" fault. (d)–(f) $P\mathrm{sgn}(t)$ with respect to time for the "abg" fault.

Fig. 6. (a)–(c) $P_1(t)$ and $P_2(t)$ with respect to time for the "abc" fault. (d)–(f) $P\mathrm{sgn}(t)$ with respect to time for the "abc" fault.
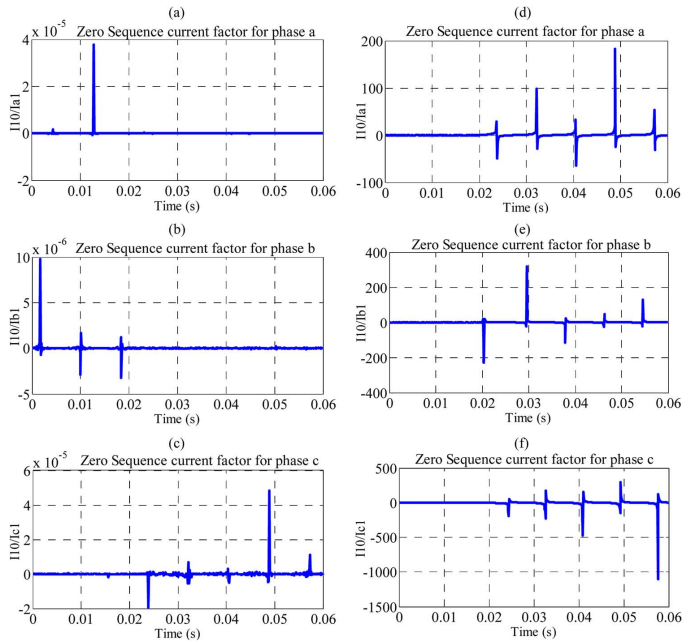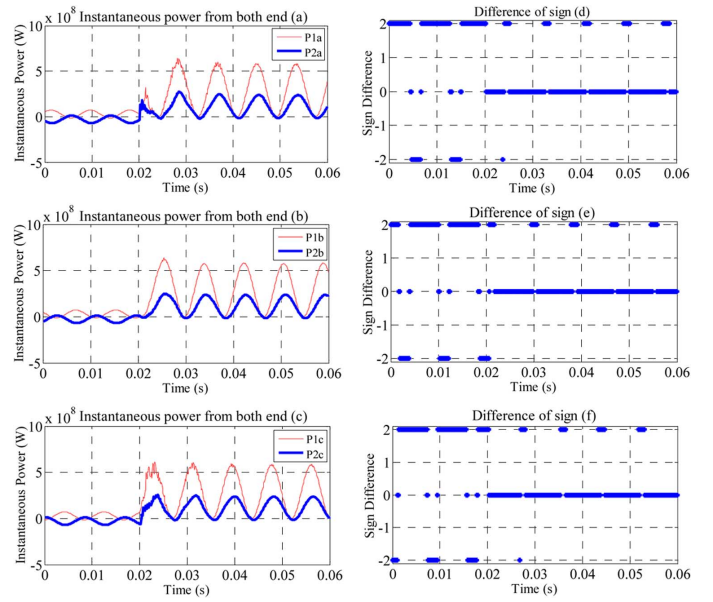

Fig. 5. (a)–(c) Zero-sequence current factors for the "ab" fault. (d)–(f) Zero-sequence current factors for the "abg" fault.

Fig. 7. (a)–(c) $P_1(t)$ and $P_2(t)$ with respect to time for the load level change. (d)–(f) $P\mathrm{sgn}(t)$ with respect to time for the load level change.

Fig. 6(a)–(c). The plot of $P\mathrm{sgn}(t)$ with respect to time is shown in Fig. 6(d)–(f). It is clear that all three phases are faulted as

$$\left|P_{1a}^{f}(t)\right| > 0, \ \left|P_{2a}^{f}(t)\right| > 0, \ \left|P_{1b}^{f}(t)\right| > 0, \ \left|P_{2b}^{f}(t)\right| > 0,$$
$$\left|P_{1c}^{f}(t)\right| > 0, \ \left|P_{2c}^{f}(t)\right| > 0.$$

4) Load Level Change: Sometimes, relay trips following overload conditions are due to a sudden change in load. In that

case, the fault detection method should not detect this change as a fault and the warning about relay misoperation should be issued. In case of load level change (one change of 100% at 0.025 s and another change of 50% over already increased the load at 0.04 s), the plot of $P_1(t)$ and $P_2(t)$ with respect to time is shown in Fig. 7(a)–(c). The plot of $P\mathrm{sgn}(t)$ with respect to time is shown in Fig. 7(d)–(f). From Fig. 7, it is clear that the line is not faulted.

5) Faults on Adjacent Line: To verify that the method is not influenced by faults on adjacent line, an "ag" fault is applied on an adjacent line and the plot of $P_1(t)$ and $P_2(t)$ with respect to time is shown in Fig. 8(a)–(c). The plot of $P\mathrm{sgn}(t)$ with respect

This article has been accepted for inclusion in a future issue of this journal. Content is final as presented, with the exception of pagination.

DUTTA *et al.*: TRANSMISSION-LINE FAULT ANALYSIS USING SYNCHRONIZED SAMPLING

5
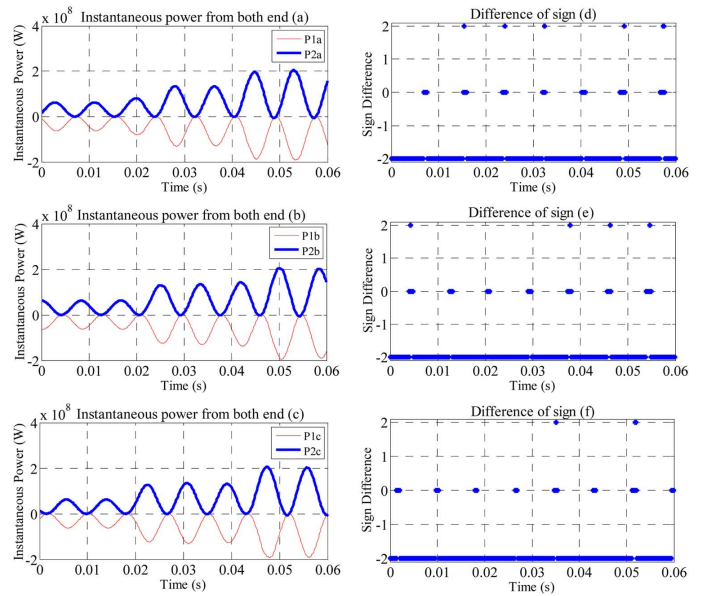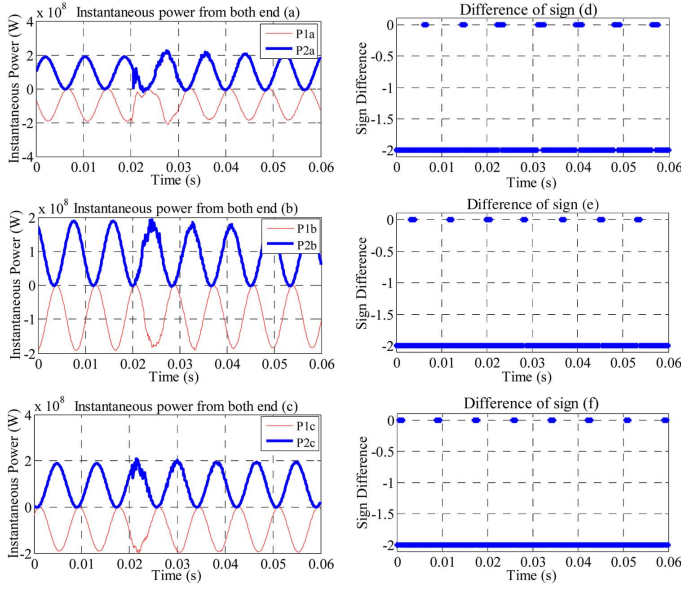

Fig. 8. (a)–(c) $P_1(t)$ and $P_2(t)$ with respect to time for the adjacent line. (d)–(f) $P\mathrm{sgn}(t)$ with respect to time for the adjacent line.
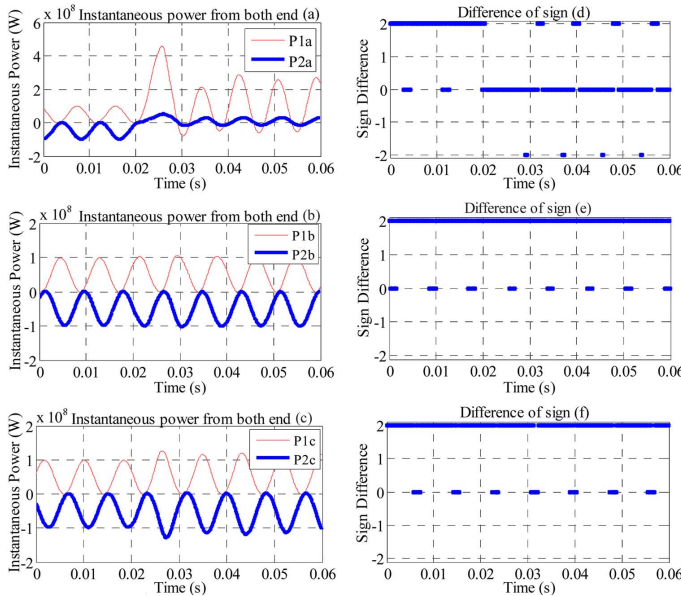

Fig. 9. (a)–(c) $P_1(t)$ and $P_2(t)$ with respect to time for the weak infeed case. (d)–(f) $P\mathrm{sgn}(t)$ with respect to time for the weak infeed case.

Fig. 10. Parallel transmission line.
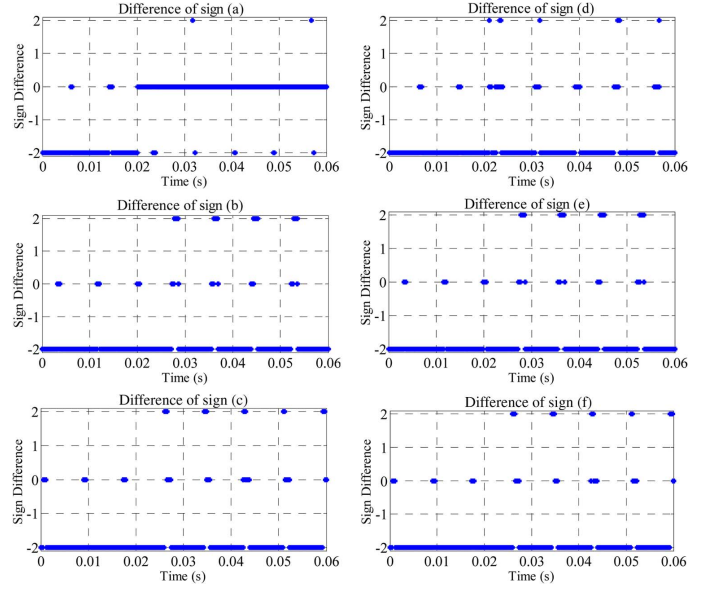
Fig. 11. (a)–(c) $P\mathrm{sgn}(t)$ with respect to time for the "ag" fault on line-1. (d)–(f) $P\mathrm{sgn}(t)$ with respect to time for the "ag" fault on line-2.

to time is shown in Fig. 8(d)–(f). From Fig. 8, it is clear that the line of interest is not influenced by faults on the adjacent line.

6) Faults Under Weak Infeed: A single-phase fault (ag) is applied on a line with weak infeed. The plots of $P_1(t)$ and $P_2(t)$ with respect to time are shown in Fig. 9(a)–(c). The plot of $P\mathrm{sgn}(t)$ with respect to time is shown in Fig. 9(d)–(f). From Fig. 9, it is clear that the proposed method can detect and classify the fault under weak infeed conditions. Since the proposed method relies on the change of direction, unless the current from weak infeed is exact zero, it is applicable. Therefore, this method is not applicable to radial distribution systems.

7) Faults on the Parallel Lines: Detection and classification of faults occurring on parallel lines (Fig. 10) either single-line

fault or cross-line fault is very difficult due to the presence of mutual coupling. If synchronous voltage and current measurements at both ends of the parallel lines are available, we can apply the proposed method to detect and classify the fault. Fig. 11(a)–(c) shows the plot of $P\mathrm{sgn}(t)$ with respect to time for one of the lines (line 1) and Fig. 11(d)–(f) shows the same for the other line (line 2) for the "ag" fault on the 1st line. It can be concluded that only one line is faulted and the other is not and the fault type is "ag" fault. For cross-line faults, both lines will be detected as faulted.

B. Fault Location

The synchronized sampling-based fault-location scheme originally proposed in [17] is used in this paper with some modifications. Once the line is detected as faulted, an accurate fault location can be identified by this method. For the short transmission line (represented using lumped parameters), the explicit form of the fault-location equation can be derived as

$$d_S = \frac{-\sum_{m=a,b,c}\sum_{k=1}^{N} P_m(k)Q_m(k)}{\sum_{m=a,b,c}\sum_{k=1}^{N} Q_m^2(k)} \qquad (6)$$
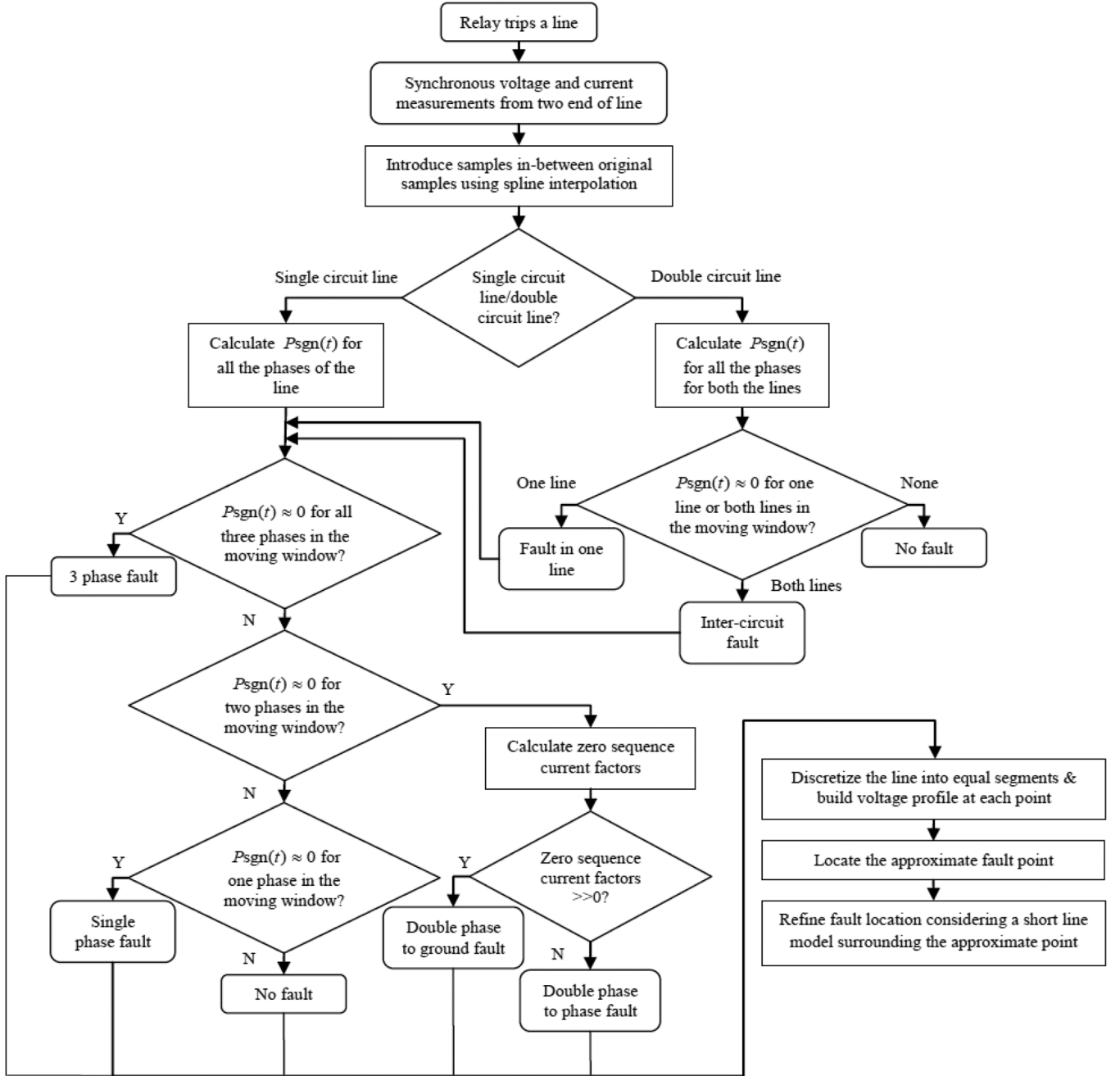
Fig. 12.   Flowchart of the proposed fault detection and classification scheme.

where

$$P_m(k) = v_{mR}(k) - v_{mS}(k)$$
$$- d \sum_{p=a,b,c} \left[\left(R_{mp} + \left(\frac{L_{mp}}{\Delta t} \right) \right) i_{pR}(k) \right.$$
$$\left. - \left(\frac{L_{mp}}{\Delta t} \right) i_{pR}(k-1) \right]$$
$$Q_m(k) = d \sum_{p=a,b,c} \left[\left(R_{mp} + \left(\frac{L_{mp}}{\Delta t} \right) \right) [i_{pR}(k) + i_{pS}(k)] \right.$$
$$\left. - \left(\frac{L_{mp}}{\Delta t} \right) [i_{pR}(k-1) + i_{pS}(k-1)] \right]$$
$$m = a, b, c$$

k is the present sample point; Δt is the time period with respect to the sampling frequency; and subscripts S and R stand for the values at the sending end and receiving end, respectively.

For long transmission lines (represented using distributed parameters), a pair of recursive equations is obtained

$$v_j(k) = \left[\left(\frac{1}{2} \right) [v_{j-1}(k-1) + v_{j-1}(k+1)] \right.$$
$$+ \left(\frac{Z_c}{2} \right) [i_{j-1}(k-1) - i_{j-1}(k+1)]$$
$$\left. + \left(\frac{R\Delta x}{4} \right) [i_{j-1}(k+1) - i_{j-1}(k-1)] \right] \quad (7)$$

This article has been accepted for inclusion in a future issue of this journal. Content is final as presented, with the exception of pagination.

DUTTA *et al.*: TRANSMISSION-LINE FAULT ANALYSIS USING SYNCHRONIZED SAMPLING

7

$$i_j(k) = \left[\left(\frac{1}{2Z_c} \right) [v_{j-1}(k-1) - v_{j-1}(k+1)] \right.$$

$$+ \left(\frac{1}{2} \right) [i_{j-1}(k-1) + i_{j-1}(k+1)]$$

$$- \left(\frac{R\Delta x}{2Z_c} \right) i_j(k)$$

$$\left. - \left(\frac{R\Delta x}{4Z_c} \right) [i_{j-1}(k-1) + i_{j-1}(k+1)] \right] \quad (8)$$

where $\Delta x = \Delta t / \sqrt{LC}$ is the distance that the wave travels with a sampling time step Δt, $Z_c = \sqrt{L/C}$ is the surge impedance, subscript j is the position of the discretized point of the line, and k is the sample point.

Since the explicit form of the fault location cannot be obtained, an indirect approach is used to calculate the final fault location as described in the following steps:

1) Discretize the line into equal segments with a length of Δx and build a voltage profile for each point calculating from the sending end and receiving end, respectively.
2) Locate the approximate fault point by finding the point that has the minimum square of voltage difference calculated from both ends.
3) Build a short line model surrounding the approximate fault point, and refine the fault location using the algorithm based on lumped line parameters.

Since the fault-location method is based on the distributed parameter line model, it requires a very high sampling rates for voltage and current signals. Since the fault detection and classification method do not require high sampling rates, the spline interpolation technique [22] is used between input samples to achieve a higher sampling rate appearance for fault-location applications.

III. IMPLEMENTATION

A flowchart for the proposed method is shown in Fig. 12. The method is initiated after a relay trips a line. Synchronized voltage and current measurements from both ends of the line are gathered. Depending on the configuration of the line (single or parallel), instantaneous powers at both ends and $P\mathrm{sgn}(t)$ are calculated for all the phases for the single line or both parallel lines. If for parallel lines $P\mathrm{sgn}(t) \approx 0$ in a 7 ms moving window for both lines, then it is crossline or intercircuit fault, if $P\mathrm{sgn}(t) \approx 0$ for only one line of the parallel lines, the fault is a single-line fault, and if $P\mathrm{sgn}(t) \neq 0$, there is no fault. If there is any fault on parallel lines, the classification procedure will be the same as in a single-line case. For the single line, if $P\mathrm{sgn}(t) \approx 0$ for all phases, the fault type is a three-phase fault, else if $P\mathrm{sgn}(t) \approx 0$ for two phases, we check for phase-phase-to-ground fault by computing zero-sequence current factors and if those factors are much more than zero, then the fault is a double-phase-to-ground fault. Otherwise, it is a phase-to-phase fault. If $P\mathrm{sgn}(t) \approx 0$ for only one phase, then fault type is a single-phase-to-ground fault and otherwise there is no fault. After the fault is detected and classified, the fault-location subroutine is performed as described in Section II-B.

TABLE I
SUMMARY OF FAULT ANALYSIS UNDER VARYING
FAULT DISTANCES AND FAULT RESISTANCES

Fault Type	Fault Location (mi)	Fault Resistance (Ω)	Actual Fault Inception Time (s)	Detected Fault Type	Calculated Fault Inception Time (s)	Time to detect (ms)	Calculated Fault Location (mi)	Fault Location % Error
ag	8.28 (5%)	0	0.02	ag	0.022	2	-	-
	33.13 (20%)			ag	0.022	2	33.84	0.43
	82.84 (50%)			ag	0.022	2	82.70	0.09
	8.28 (5%)	20	0.02	ag	0.022	2	-	-
	33.13 (20%)			ag	0.024	4	33.84	0.43
	82.84 (50%)			ag	0.022	2	82.70	0.09
	8.28 (5%)	100	0.02	ag	0.022	2	9.14	0.52
	33.13 (20%)			ag	0.022	2	33.82	0.41
	82.84 (50%)			ag	0.022	2	82.70	0.09
ab	8.28 (5%)	0	0.02	ab	0.027	7	12.02	2.26
	33.13 (20%)			ab	0.023	3	33.26	0.08
	82.84 (50%)			ab	0.023	3	82.52	0.19
abg	8.28 (5%)	0	0.02	abg	0.027	7	12.02	2.26
	33.13 (20%)			abg	0.023	3	33.26	0.08
	82.84 (50%)			abg	0.023	3	82.52	0.19
	8.28 (5%)	20	0.02	abg	0.023	3	10.06	1.08
	33.13 (20%)			abg	0.023	3	33.54	0.24
	82.84 (50%)			abg	0.023	3	82.54	0.18
	8.28 (5%)	100	0.02	abg	0.023	3	10.73	1.48
	33.13 (20%)			abg	0.023	3	33.06	0.05
	82.84 (50%)			abg	0.023	3	82.46	0.23
abc	8.28 (5%)	0	0.02	abc	0.024	4	-	-
	33.13 (20%)			abc	0.024	4	37.62	2.71
	82.84 (50%)			abc	0.023	3	83.90	0.64
	8.28 (5%)	20	0.02	abc	0.023	3	8.07	0.13
	33.13 (20%)			abc	0.023	3	38.01	2.94
	82.84 (50%)			abc	0.023	3	82.83	0.004
	8.28 (5%)	100	0.02	abc	0.023	3	13.12	2.92
	33.13 (20%)			abc	0.023	3	45.03	7.18
	82.84 (50%)			abc	0.023	3	82.61	0.14

IV. TEST RESULTS

The proposed method is tested for several simulated cases on lines 30–38 of the IEEE 118-bus test system. The line length is 165 miles. The test system is modeled in ATP Draw [23] and different types of faults under different conditions are simulated and synchronized voltage and current signal samples prefault and postfault at both ends of the line are used to verify the algorithm. The sampling frequency for voltage and current measurements is 1 kHz. The following subsections contain the results under different conditions.

A. Changing Fault Distance

The distance to fault from one end of a line is changed to 5%, 20%, and 50% of the line length with fault resistance changes 0, 20, and 100 Ω. Table I provides the summary of the results for different types of faults under varying fault distance and resistance. The proposed method detects and classifies a fault using a 7 ms data window after fault inception on the postfault data. Fault-location accuracy is within 3% except for one case. Table II shows the summary of the results of single-line-to-ground faults under very high fault resistance. High-resistance fault cases are extremely rare for other fault types.

B. Changing Fault Inception Angle

A fault inception angle in degrees is changed to 0°, 40, 80, 120, and 160°. Table III provides the summary of the results for different types of fault under varying fault inception angles. The proposed method detects and classifies faults within 7 ms for all types of faults. Fault-location accuracy is within 3%.

This article has been accepted for inclusion in a future issue of this journal. Content is final as presented, with the exception of pagination.

8   IEEE TRANSACTIONS ON POWER DELIVERY

TABLE II
SUMMARY OF FAULT ANALYSIS FOR HIGH-RESISTANCE FAULTS

Fault Location (mi)	Fault Resistance (Ω)	Actual Fault Inception Time (s)	Calculated Fault Inception Time (s)	Time to detect (ms)	Calculated Fault Location (mi)	Fault Location % Error
8.28 (5%)			0.024	4	9.09	0.49
33.13 (20%)	200	0.02	0.024	4	33.79	0.4
82.84 (50%)			0.024	4	82.71	0.08
8.28 (5%)			0.023	3	9.02	0.45
33.13 (20%)	500	0.02	0.024	4	33.73	0.36
82.84 (50%)			0.024	4	82.74	0.06
8.28 (5%)			0.022	2	8.98	0.42
33.13 (20%)	1000	0.02	0.022	2	33.66	0.31
82.84 (50%)			0.022	2	82.78	0.04
8.28 (5%)			0.022	2	8.93	0.39
33.13 (20%)	10000	0.02	0.022	2	33.38	0.15
82.84 (50%)			0.022	2	82.79	0.03

TABLE III
SUMMARY OF FAULT ANALYSIS UNDER A VARYING FAULT INCEPTION ANGLE

Fault Type	Fault Location (mi)	Fault Inception Angle (degree)	Actual Fault Inception Time (s)	Detected Fault Type	Calculated Fault Inception Time (s)	Time to detect (ms)	Calculated Fault Location (mi)	Fault Location % Error
ag	33.13 (20%)	0	0.02	ag	0.024	4	33.84	0.43
		40	0.0218	ag	0.025	3.1	34.57	0.87
		80	0.0237	ag	0.03	6.2	35.59	1.48
		120	0.0255	ag	0.03	4.5	35.44	1.39
		160	0.0274	ag	0.033	5.6	34.54	0.85
	82.84 (50%)	0	0.02	ag	0.024	4	82.70	0.09
		40	0.0218	ag	0.025	3.1	82.64	0.12
		80	0.0237	ag	0.028	4.2	82.62	0.13
		120	0.0255	ag	0.03	4.5	82.56	0.17
		160	0.0274	ag	0.033	5.6	82.69	0.09
ab	33.13 (20%)	0	0.02	ab	0.023	3	34.16	0.62
		40	0.0218	ab	0.025	3.2	36.47	2.02
		80	0.0237	ab	0.029	5.3	32.71	0.26
		120	0.0255	ab	0.031	5.5	32.29	0.51
		160	0.0274	ab	0.031	3.6	32.84	0.18
	82.84 (50%)	0	0.02	ab	0.023	3	82.94	0.06
		40	0.0218	ab	0.025	3.2	82.80	0.02
		80	0.0237	ab	0.028	4.3	82.08	0.46
		120	0.0255	ab	0.03	4.5	82.78	0.04
		160	0.0274	ab	0.031	3.6	82.93	0.05
abg	33.13 (20%)	0	0.02	abg	0.023	3	33.54	0.24
		40	0.0218	abg	0.025	3.2	34.00	0.52
		80	0.0237	abg	0.03	6.3	34.05	0.55
		120	0.0255	abg	0.031	5.5	34.75	0.98
		160	0.0274	abg	0.031	3.6	35.14	1.21
	82.84 (50%)	0	0.02	abg	0.023	3	82.54	0.18
		40	0.0218	abg	0.025	3.2	82.70	0.08
		80	0.0237	abg	0.028	4.3	82.66	0.11
		120	0.0255	abg	0.031	5.5	82.94	0.06
		160	0.0274	abg	0.031	3.6	82.56	0.17
abc	33.13 (20%)	0	0.02	abc	0.023	3	38.01	2.94
		40	0.0218	abc	0.025	3.2	33.53	0.24
		80	0.0237	abc	0.028	4.3	30.23	1.75
		120	0.0255	abc	0.029	3.5	32.40	0.44
		160	0.0274	abc	0.031	3.6	31.26	1.13
	82.84 (50%)	0	0.02	abc	0.023	3	82.83	0.00
		40	0.0218	abc	0.025	3.2	82.55	0.18
		80	0.0237	abc	0.028	4.3	82.67	0.10
		120	0.0255	abc	0.029	3.5	82.96	0.07
		160	0.0274	abc	0.031	3.6	83.40	0.34

V. CONCLUSIONS

A simple yet efficient fault analysis method to detect, classify, and locate transmission-line faults using synchronized samples of voltage and current from both (all) transmission-line ends is proposed. The proposed method has the following features.

- It detects and classifies faults very accurately and quickly. Using pre-event and postevent samples, it can detect whether the disturbance is a fault within 7 ms of event inception.
- It does not require elaborate parameter settings for detection thresholds.

- It is transparent to the effects of fault resistance and the use of transmission-line models, which makes it very easy to implement.
- The method depends on accurate representation of a transmission-line model and, therefore, produces very accurate fault-location results.
- Due to the presence of modern circuit breakers opening in less than two cycles, a limited postfault waveform signal is available to be captured by the recorders, and this method is applicable in that situation.
- The method is tested for several fault cases varying fault distance, fault resistance, and fault inception angle simulated in an IEEE test case, and accurate fault detection, classification, and location are demonstrated.
- The method can successfully detect and classify which line is faulted in the case of parallel lines and can even detect cross-line faults. For the location part, only the line which is faulted is used to estimate the location.
- The method can discriminate load level changes from fault cases, and it can be used to validate relay trip decisions.

REFERENCES

[1] M. S. Sachdev and M. A. Baribeau, "A new algorithm for digital impedance relays," *IEEE Trans. Power App. Syst.*, vol. PAS–98, no. 6, pp. 2232–2239, Dec. 1979.
[2] A. A. Girgis, "A new Kalman filtering based digital distance relay," *IEEE Trans. Power App. Syst.*, vol. PAS–101, no. 9, pp. 3471–3480, Sep. 1982.
[3] M. Kezunovic, I. Rikalo, and D. J. Sobajic, "High speed fault detection and classification with neural nets," *Elect. Power Syst. Res. J.*, vol. 34, no. 2, pp. 109–116, Aug. 1995.
[4] N. Zhang and M. Kezunovic, "Coordinating fuzzy ART neural networks to improve transmission line fault detection and classification," presented at the IEEE Power Energy Soc. Gen. Meeting, San Francisco, CA, USA, Jun. 2005.
[5] B. Das and J. V. Reddy, "Fuzzy logic based fault classification scheme for digital distance protection," *IEEE Trans. Power Del.*, vol. 20, no. 2, pt. 1, pp. 609–616, Apr. 2005.
[6] O. A. S. Youssef, "Combined fuzzy-logic wavelet-based fault classification technique for power system relaying," *IEEE Trans. Power Del.*, vol. 19, no. 2, pp. 582–589, Apr. 2004.
[7] B. Mahamedi, "A novel setting-free method for fault classification and faulty phase selection by using a pilot scheme," presented at the 2nd Int. Conf. Elect. Power Energy Convers. Syst., Sharjah, United Arab Emirates, 2011.
[8] M. Kezunovic and B. Perunicic, "Fault Location," in *Wiley Encyclopedia of Electrical and Electronics Terminology*. New York, USA: Wiley, 1999, vol. 7, pp. 276–285.
[9] *IEEE Guide for Determining Fault Location on the Transmission and Distribution Lines*, IEEE C37.144-2004.
[10] T. Takagi, Y. Yamakoshi, M. Yamaura, R. Kondow, and T. Matsushima, "Development of a new type fault locator using the one-terminal voltage and current data," *IEEE Trans. Power App. Syst.*, vol. PAS-101, no. 8, pp. 2892–2898, Aug. 1982.
[11] L. Eriksson, M. Saha, and G. D. Rockefeller, "An accurate fault locator with compensation for apparent reactance in the fault resistance resulting from remote end infeed," *IEEE Trans. Power App. Syst.*, vol. PAS-104, no. 2, pp. 424–436, Feb. 1985.
[12] J. Izykowski, E. Rosolowski, and M. M. Saha, "Locating faults in parallel transmission lines under availability of complete measurements at one end," *Proc. Inst. Elect. Eng., Gen., Transm. Distrib.*, vol. 151, no. 2, pp. 268–273, Mar. 2004.
[13] A. Johns and S. Jamali, "Accurate fault location technique for power transmission lines," *Proc. Inst. Elect. Eng., Gen., Transm. Distrib.*, vol. 137, no. 6, pp. 395–402, Nov. 1990.
[14] D. Novosel, D. G. Hart, E. Udren, and J. Garitty, "Unsynchronized two-terminal fault location estimation," *IEEE Trans. Power Del.*, vol. 11, no. 1, pp. 130–138, Jan. 1996.